Transactions of the **13th International Conference on Structural Mechanics in Reactor Technology** (SMiRT 13), Escola de Engenharia - Universidade Federal do Rio Grande do Sul, Porto Alegre, Brazil, August 13-18, 1995

Stress assessment of a component using 3D finite element models

Mattar Neto, M., Miranda, C.A.J., Cruz, J.R.B., Bezerra, L.M.
Comissão Nacional de Energia Nuclear/SP-IPEN, São Paulo, SP, Brazil

ABSTRACT: The evaluation of components using three dimensional (3D) finite element analysis (FEA) does not generally fall into the shell type verification. Consequently, the demonstration that the modes of failure are avoided sometimes is not straightforward. Elastic rules, developed by limit load theory, require the computation of the shell type through wall membrane and bending stresses. How to calculate these stresses from 3D FEA is not necessarily self-evident. One approach to be considered is to develop recommendations in a case-by-case basis for the most common pressure vessel geometries and loads based on comparison between the results of elastic and also plastic FEA. In this paper the case of a complex geometry - lugs attached to a cylindrical pressure vessel wall - is examined and discussed. This case is typically a three-dimensional (3D) configuration where it is not a simple task to check the requirements of the ASME code. From the comparison of the results of 3D elastic and elastic-plastic FEA some conclusions are addressed.

1 INTRODUCTION

The main standard for the design of nuclear pressure vessels and piping is the ASME code (ASME, 1992). In the whole world, such code is simply adopted, fitted, or copied into requirements as the major criterion for pressure vessel design. In the early 60's, the ASME recognized with considerable foresight, the advantages to be gained from detailed stress analysis. Thereupon, the ASME introduced the so-called "design by analysis" route which was deliberately set up for nuclear applications (ASME, 1969).

The rules formulated in the "design by analysis" approach were based upon concepts from plasticity in an attempt to avoid mainly the consequences of possible bursting or ratcheting failure and fatigue. This approach required an elastic analysis of the vessel or component (although it did not restrict design to elastic analysis alone) and the separation and classification of the calculated shell type stresses. The stresses were categorized into primary, secondary, and peak stresses and different design allowables were applied according to the failure mode to be avoided.

the method of stress calculation was mot specified, although it was clear at the time that shell discontinuity analysis was seen as the main method of analysis. The dominant problem in "design by analysis" is that of categorization of stresses. The rules governing stress categorization are not precise, but experience and common practice coupled with

the use of thin shell calculations have allowed some degree of reliability to be introduced into the design process.

However, if the elastic analysis is performed using more detailed continuum finite element calculations, which is a very common practice today, then the categorization of the stresses and the extraction of shell type through wall membrane and bending stresses, primary and primary plus secondary, become fraught with difficulty.

Both primary and primary plus secondary stress limits involve transition from elasticity to plasticity. Using limit load theory, elastic limits are readily defined for simple structures under simple loading (e.g. beams under tension or bending loads). Also, shells of revolution can be reasonably evaluated for elastic limits. Once the elastic limits are known, guidelines can be written for performing elastic analysis that assures conservatism while giving reasonably accurate solutions relative to the limit load solution. Once the guidelines are established, the designer can clearly demonstrate that the limits on the modes of failure have been met.

2 MOTIVATION

The evaluation of components using three dimensional (3D) finite element analysis (FEA) does not generally fall into the shell type verification cookbook. Consequently, the demonstration that the modes of failure are avoided sometimes is not straightforward. Elastic rules, developed by limit load theory, require the computation of the shell type through wall membrane and bending stresses. How to calculate these stresses from 3D FEA is not necessarily self-evident. The general opinion of pressure vessel designers is that current techniques can provide safety comparable to current axisymmetric evaluations. These common approaches appear to be based more on a hoped-for conservatism rather than accuracy.

The ASME code gives some limited guidance in this area for a few specific geometries and loads; these are generally adequate for axisymmetric conditions. When the analysis switches from axisymmetric assumptions to 3D, code guidelines become more difficult to apply. For these cases, the need for better guidelines or rules seems to be justifiable.

The expectation that the widespread use of FEA would displace more simplified methods of analysis in pressure vessel and piping design was not confirmed. On the contrary, the need for simplified methods had become even greater. The main reason for this trend is that FEA (axisymmetric and 3D) generates results that often need expertise to reinterpret them in order to make engineering assessments and stress evaluations.

The main question to be answered is how to assess the structural design of pressure vessels from an elastic FEA considering that the failure modes to be avoided are closely related to plastic (nonlinear) effects

One approach to be considered is to develop recommendations in a case-by-case basis for the most common pressure vessels geometries and loads based on comparison between the results of elastic and also plastic FEA. This proposal is indicated in Hollinger and Hechmer (1994) considering that ASME code assessment of stress limits for complex geometries and loading conditions requires a clear understanding of the relationship between stress categories and failure mechanism relation to them, the appropriate stresses for each stress category, the appropriate locations for assessing stresses, and the approach used to calculate membrane plus bending stresses (to linearize stresses) in FEA.

In this paper, following the indication given in Hollinger and Hechmer (1994), the case

of a complex geometry - lugs attached to a cylindrical pressure vessel wall - is examined and discussed. This case is typically a 3D configuration where it is not a simple task to check the requirements of the ASME code. From the comparison of the results of 3D elastic and elastic-plastic FEA some conclusions are addressed.

3 THE STUDIED CASES

The studied cases of this paper concern a cylindrical pressure vessel with two symmetric radial lugs under different loading conditions. Finite element models taking advantage of the symmetries of geometry and loading are considered for the elastic and elastic-plastic analyses. The applied loads considered in the analyses are: internal pressure in the cylindrical shell, and radial and axial forces acting on the lugs. The forces directions refer to the cylindrical shell coordinate system. The geometric and material characteristics of the region of the lug-cylinder attachment are presented in Figure 1 together with one of the finite element models used for the stress analyses.

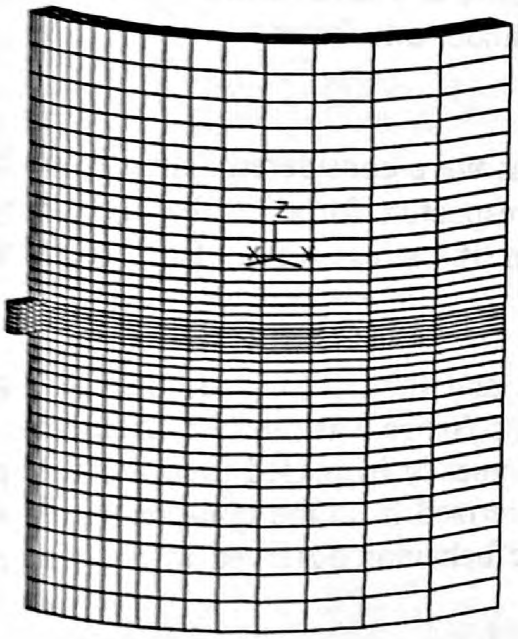

cylinder inner radius = 1000 mm
cylinder thickness = 100 mm
dimensions of the lugs =100x100x100 mm

Figure 1: General dimensions and one of the finite element models of the lug-cylinder attachment

4 FEA

Two finite element models were built for the stress analyses. The first model can be seen in Figure 1 and was used for the stress evaluation of the structure under internal pressure plus the axial force on each lug. In this case, taking credit of the cylinder-lugs attachment symmetry and the symmetry of the axial force, only a quarter of the structure was discretized.

For the evaluation of the structure under internal pressure and the radial force on the lug, the model of Figure 2 was used, taking credit again of the symmetry of geometry and loads.

Two different models with different discretization were used for the analyses although

it is known that a single model with different boundary conditions could be used to perform all of them.

Solid elements with eight nodes and three degrees of freedom per node were used in the FEA. Elastic and elastic-plastic analyses were undertaken with the help of the ANSYS software package, version 5.0A (SASI 1992). The material properties used in FEA were: E = 200000 MPa as the Young's modulus, $\nu = 0.3$ as the Poisson's ratio, $\sigma_y = 276$ MPa as the yielding stress and $S_m = 184$ MPa as the design stress intensity value. In the elastic-plastic FEA it was assumed perfect plasticity with no strain hardening.

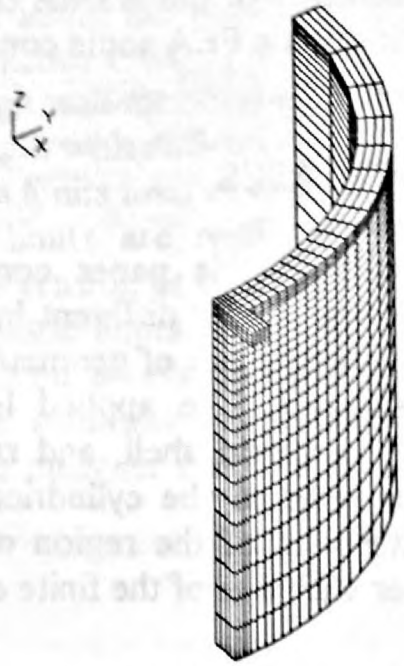

Figure 2: Finite element model of the lug-cylinder attachment

In the elastic analyses, two separate load cases were considered acting in each model corresponding to the internal pressure and the respective force on the lug. Using stress post-processor available in the ANSYS program, the stress results from each load step were combined employing appropriate factors for each load step.

In the elastic-plastic analyses, two situations were evaluated for each model. In the first, the internal pressure was initially applied and then the forces on the lugs were successive and monotonically increased until the collapse was reached. In the other, only the forces on the lugs were applied and monotonically increased until the collapse was reached. The elastic-plastic collapse was characterized from the non-convergence of the finite element solution and from the asymptotic behavior observed in the displacement versus applied force curve.

5 RESULTS

From the elastic-plastic FEA results, the forces on the lugs that cause the collapse of the lug-cylinder attachment can be summarized in Table 1.

Table 1: Collapse forces in the lugs (MN), from elastic-plastic FEA

Radial forces in the lugs	with internal pressure	2.72
	without internal pressure	2.65
Axial forces in the lugs	with internal pressure	1.58
	without internal pressure	1.53

The distribution of the stress intensities for the collapse load combinations are shown in Figures 3 to 6 for each load case, respectively, analyzed in this paper. In the case of axial force on the lug, one can observe that the high stresses are very localized. The high stress values are concentrated in the region of the gross geometric discontinuity between the lug and the cylinder. It is noticed that the failure did not take place nor in the lug or in the cylinder but in the shell-lug intersection. On the other hand, in the case of the radial forces acting on the lug, high stress values are present in the cylinder. Of course, this state of high stress distribution in the shell is largely influenced by the lug load and due to the strength of the cylinder wall resisting the throughout punching of the lug. The strength of the cylinder wall, stopping the radial deformation of the lug, is shown by the radial deformation of the shell. Such deformation gives rise to high bending stresses. In this case, the high stress state observed in the cylinder wall led the cylinder to failure not the lug. There are differences in the behavior of the cylinder when the lug is under axial or radial forces. The different behavior may be explained by the fact that the lug forces in different directions strengthen the shell also in different ways. More membrane stresses in the cylinder is achieved to resist the axial lug force while more bending stresses resist the radial lug force.

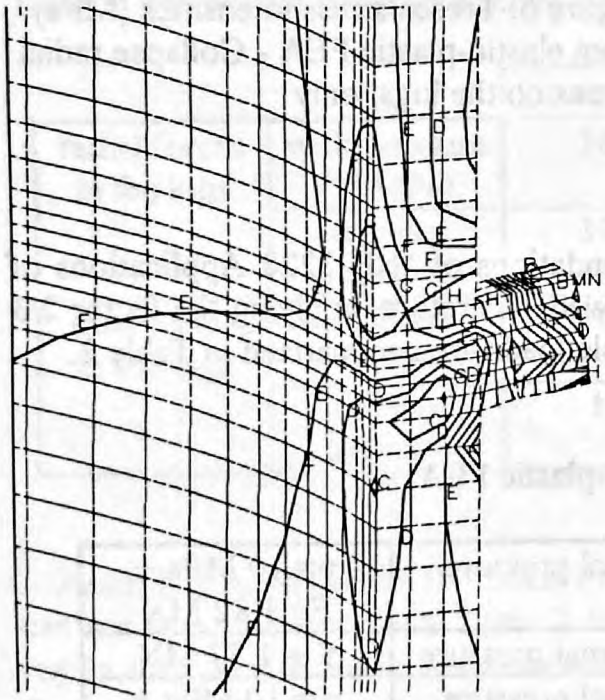

A = 56 MPa to I = 288 MPa

Figure 3: Tresca stress intensities (MPa) from elastic-plastic FEA - Collapse axial forces on the lugs plus internal pressure (15 MPa)

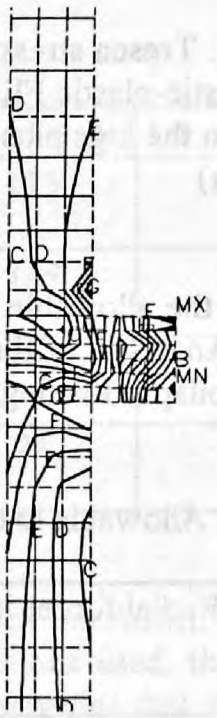

A = 57 MPa to I = 288 MPa

Figure 4: Tresca stress intensities (MPa) from elastic-plastic FEA - Collapse axial forces on the lugs, only

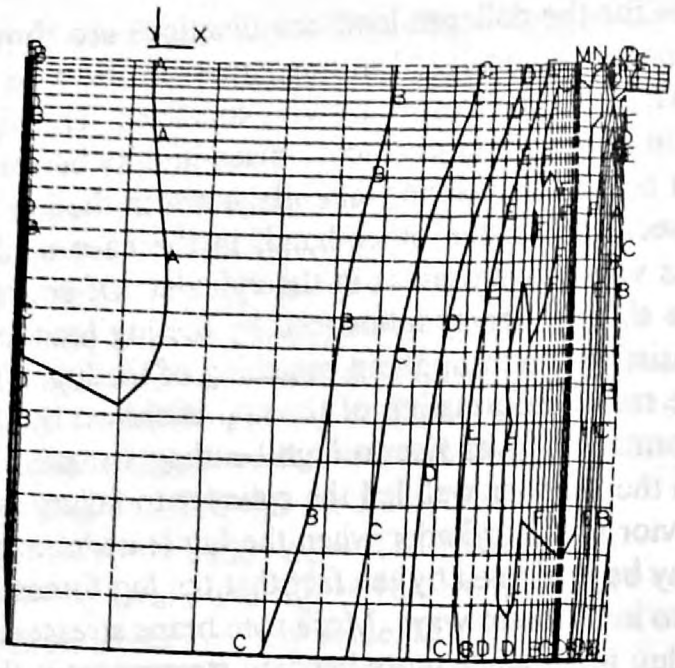

A = 43 MPa to F = 310 MPa

Figure 5: Tresca stress intensities (MPa) from elastic-plastic FEA - Collapse radial forces on the lugs plus internal pressure (15 MPa)

A = 45 MPa to F = 290 MPa

Figure 6: Tresca stress intensities (MPa) from elastic-plastic FEA - Collapse radial forces on the lugs, only

To find the allowable load value, the recommendations of "NB-3228 Applications of Plastic Analysis" of the ASME code were followed. Therefore, applying the factor 2/3 to the collapse loading combination, the allowable loads are summarized in Table 2.

Table 2: Allowable load conditions, from elastic-plastic FEA

Radial forces in the lugs	with internal pressure	p= 10 MPa + F= 1.82 MN
	without internal pressure	F = 1.77 MN
Axial forces in the lugs	with internal pressure	p = 10 MPa + F = 1.05 MN
	without internal pressure	F = 1.02 MN

If the designer uses a simple elastic FE analysis to evaluate the shear in the lugs and in the shell, the recommendations of "NB-3227.2 Pure Shear" of the ASME code have to be followed. In this situation, the allowable forces in the lugs are 4.42 MN and 1.11 MN for the radial and the axial directions, respectively. Notice that those allowable forces were found considering the average shearing stresses on the strength sections of the structure. The shearing stresses correspond to the situation of the lug punching the shell for the lug under radial force and the lug tearing out from the shell for the lug under axial force.

Comparing those results with the values from Table 2 one may conclude that the

simplified elastic analysis shows good agreement in the case more close to pure shear which corresponds to the axial force on the lug. In the situation of shell punching (radial forces on the lug) the results do not agree. In this case it can be concluded that the elastic analysis may lead to non-conservative design.

To compare the results from elastic and elastic-plastic FEA it is necessary to define the loads from elastic FEA corresponding to the allowable stress limits prescribed by the ASME code. Therefore, in the case of elastic FEA, it is always necessary to separate and classify the finite element stresses in shell type stresses. In other words, the FE stresses have to be divided and categorized into wall membrane and bending stresses. However, as mentioned in the Introduction of this paper, there is no established procedure to perform this categorization in 3D finite element models. In this work, it was followed the recommendations of Hechmer and Holliger (1991) and the so-called "linearization by a line". The lines (L) were chosen at the shell body and at distances away from the edge of the lug attachment. The distances were taken as $0.1\sqrt{Rt}$, $0.5\sqrt{Rt}$, $1.0\sqrt{Rt}$, and $2.0\sqrt{Rt}$, respectively for the lines L1, L2, L3, and L4. R is the mean radius of shell, and t its thickness. Applying the load conditions shown in Table 2, from the elastic analyses, the membrane stress intensities shown in Table 3 can be obtained. .

Table 3: Membrane stress intensities (MPa), from elastic FEA

		L1 - $0.1\sqrt{Rt}$	L2 - $0.5\sqrt{Rt}$	L3 - $1.0\sqrt{Rt}$	L4 - $2.0\sqrt{Rt}$
radial forces in the lugs	with pressure (10MPa)	347	141	115	149
	without pressure	377	202	124	54
axial forces in the lugs	with pressure (10 MPa)	105	107	108	131
	without pressure	16	18	24	54

According to NB-3213.10 "Local Primary Membrane Stress" of the ASME code, one can see from the results of Table 3 that, for the loading conditions used, the stressed region may be considered local because the membrane stress intensities that exceed 1.1 S_m = 202 MPa do not extend more than $1.0\sqrt{Rt}$. The forces in the lugs may even be increased and the condition to consider the region as a place of local membrane stress remains satisfied. For example, in the case of radial force only, the value may be increased from 2.65 MN to 2.89 MN = (1.77/124)x1.1 S_m.

In the cases of axial forces in the lugs, the stresses in the shell are little influenced by the gross geometric discontinuity between lug and shell. As we are more concerned with the shell evaluation and the stresses in the shell due to the lug axial force is negligible, no more results and comparisons concerning this case will be presented.

With the elastic evaluation of the stresses in the local region, the radial forces in the lugs, corresponding to different stress assessment lines, can be estimated. The estimated radial forces are shown in Table 4. For instance, for the stress assessment line L1 at a distance of $0.1\sqrt{Rt}$, the radial force of 1.77 MN on the lug (disregarding the internal pressure in the cylinder) causes a stress intensity of 377 MPa. Classifying such stress as

P_L (local primary membrane stress) and, limiting it to the allowable stress limit of 1.5 S_m = 276MPa, the estimated allowable radial force turns out to be 1.30 MN = (276/377) x 1.77.

Table 4: Allowable radial forces, from elastic FEA (membrane stress as P_L)

		L1 - $0.1\sqrt{Rt}$	L2 - $0.5\sqrt{Rt}$	L3 - $1.0\sqrt{Rt}$
radial forces in the lugs	with pressure (10 MPa)	1.47	3.57	4.51
	without pressure	1.30	2.42	3.94

From the elastic FEA and considering the same loading conditions described in Table 2, the membrane plus bending stress intensities reported in Table 5 can be figured out.

Table 5: Membrane plus bending stress intensities (MPa), from elastic FEA

		L1 - $0.1\sqrt{Rt}$	L2 - $0.5\sqrt{Rt}$	L3 - $1.0\sqrt{Rt}$	L4 - $2.0\sqrt{Rt}$
radial forces in the lugs	with pressure (10 MPa)	1444	952	803	682
	without pressure	1541	971	705	568

Considering the membrane plus bending stress intensities classified in the local region as $P_L \pm P_B$ (local primary membrane plus bending stress) with the corresponding ASME allowable limit of 1.5 S_m = 276 MPa, one can evaluate the allowable radial forces from elastic FEA using the same procedure described above. The results are summarized in Table 6.

Table 6: Allowable radial forces from elastic FEA (membrane plus bending as $P_L \pm P_B$)

		L1 - $0.1\sqrt{Rt}$	L2 - $0.5\sqrt{Rt}$	L3 - $1.0\sqrt{Rt}$
radial forces in the lugs	with pressure (10 MPa)	0.36	0.54	0.63
	without pressure	0.32	0.50	0.69

If one considers the membrane plus bending stress intensities classified as P + Q (primary plus secondary stress) with the limit 3.0 S_m = 552 MPa the resultant allowable radial force on the lug are calculated and the results shown in Table 7.

Table 7: Allowable radial forces from elastic FEA (membrane plus bending as P + Q)

		L1 - $0.1\sqrt{Rt}$	L2 - $0.5\sqrt{Rt}$	L3 - $1.0\sqrt{Rt}$
radial forces in the lugs	with pressure (10 MPa)	0.72	1.08	1.26
	without pressure	0.63	1.01	1.39

6 CONCLUSIONS

This paper has presented the results of elastic and elastic-plastic 3D finite element analyses directed towards the calculation of allowable loads in a lug-cylinder configuration. Depending on the stress assessment and stress classification adopted for the elastic results interpretations, different allowable loads are obtained. In addition, taking the ASME definition of limit-load analysis as the basis for design the following conclusions could be drawn:

(a) Axial forces on the lugs have little influence in the stress distribution in the shell. (b) The allowable axial forces in the lugs considering a simplified elastic analysis - and the recomendations prescribed in the limits of "NB-3227.2 Pure Shear" of the ASME code - give good agreement with the allowable axial force obtained from the elastic-plastic FEA - with the limits of "NB-3228 Applications of Plastic Analysis" of the ASME code. In fact, 1.05 MN for the elastic analysis against 1.11 MN for the elastic-plastic FEA. (c) For the radial force on the lug, performing the same type of comparison as done in "b," did not yield good agreement - 4.42 MN (elastic) versus 1.77 MN (plastic). (d) From elastic FEA, the allowable radial forces in the lugs - obtained from the stress assessment lines near $0.1\sqrt{Rt}$ away from the edge of the lug-cylinder attachment, and considering the membrane stresses as P_L with the limit of 1.5 S_m - are about 70-80 % of the allowable force obtained from elastic-plastic FEA. This is the assessment line where the radial allowable force is better approximated when considering elastic and elastic-plastic FEA. (e) The comparison in terms of membrane plus bending stresses indicates that the results of elastic FEA are much smaller than those from elastic-plastic FEA.

The results obtained in this paper suggest that for the cases here studied the use of elastic analysis and the limits of the ASME code are conservative when compared with elastic-plastic analysis checks. The different results, however, revealed the lack of appropriate guidelines in the ASME recommendations for appropriate stress assessment and verification of complex 3D geometries. In the present stage of automation, where the engineering offices use massive FE computation, including 3D modeling for design and analysis of pressure vessel components, it is wise that ASME should develop, at least in a general sense, recomendations to guide the stress analyst to safety decisions.

REFERENCES

ASME 1992. ASME Boiler and Pressure Vessel Code, Section III, Nuclear Power Plant Components. New York:ASME.

ASME 1969. Criteria of the ASME Boiler and Pressure Vessel Code for Design by Analysis in Section III and Section VIII, Division 2. New York:ASME.

Hechmer, J. L. & G. L. Hollinger 1991. *Three Dimensional Stress Criteria. Codes and Standards and Applications for Design and Analysis of pressure Vessel and Piping Components*: 181-191. New York: ASME.

Hollinger, G. L. & J. L. Hechmer 1994. *Three Dimensional Stress Evaluation Guidelines Progress Report. Recertification and Stress Classification Issues*: 95-102. New York: ASME.

SASI 1992. *ANSYS User's Manual for revision 5.0*. Houston, PA, USA: SASI.